Quantifying stable hangingwall spans between support units

by A. Daehnke*, M.D.G. Salamon†, and M.K.C. Roberts*

Synopsis

The current methodology to design stope support systems in South African gold and platinum mines is based upon the tributary area concept. The discontinuous nature of the hangingwall rock is not adequately addressed, and mechanisms leading to rock mass failures between adjacent support units are poorly understood. The work reported here aims to formulate a basis for quantifying support mechanisms and gain insights into the influence of rock discontinuities on stable hangingwall spans.

Numerical models are used to qualitatively investigate the stress transfer from the support units to the discontinuous hangingwall. Stable hangingwall spans are quantified by considering two failure mechanisms, namely (i) beam buckling, and (ii) shear failure due to slip at the abutments.

The output of the proposed design methodology is appropriate site specific support spacing, based on discontinuity spacing and orientation. The method is particularly suited to mines at intermediate and great depth, where typically the hangingwall is highly discontinuous due to face parallel mining induced fractures. Results of parametric studies show that with increasing *in situ* compressive hangingwall stress, beam thickness and friction angle, hangingwall stability is increased, leading to wider stable hangingwall spans between adjacent support units.

Introduction

Rock mass instabilities represent the single largest cause of injuries and fatalities suffered by the workforce in the gold and platinum mines of South Africa. Approximately half of all rock related fatalities are associated with rockfalls, whilst the remainder arise from the failure of dynamically loaded rock as a consequence of seismic events (rockbursts).

Stope support systems, consisting of props and packs, are used to stabilise the rock mass surrounding the mining excavations and reduce the risk of rockfalls and rockbursts. In South African gold and platinum mines, the methodology currently used to design stope support is based upon the tributary area concept. Here a given weight of rock, determined by an area in the plane of the reef and the height of a possible fall, or the 'fall-out height', is divided between a fixed number of support elements according to the attributable area. The area is determined by the face layout and the fall-out height is presumed to be known from previous observations.

This simple concept takes care of the equilibrium requirements in a rudimentary sense, but it does not adequately address the fact that the rock being supported is likely to be fractured and jointed. Clearly, in these circumstances, the distribution of the support elements may be of paramount importance. Relatively little progress has been made in quantifying the effect of support spacing on the rock mass stability. At present, it is the responsibility of the rock engineer to estimate support spacing based upon past experience. In order to improve safety and continue mining at increasing depth, it is important to improve the understanding of the mechanisms involved in the support – rock interaction, the zones of support influence and the role of rock mass discontinuities. Past experience indicates that the ultimate solution to this problem can be achieved only if the research is approached pragmatically. The tributary area concept was the first step along a road that will have to be travelled step by step, if better hangingwall control is to be achieved in the stopes, the most vulnerable areas of the mines.

The present objective is to propose more advanced support mechanisms, specifically, to gain a deeper insight into the influence of rock discontinuities such as joints, fractures and bedding planes on 'safe' or 'stable' spans. Instabilities generally initiate at discontinuities in the hangingwall. These planes of weakness are shown to be of prime importance when spacing support units. An attempt is made in the sequel to evaluate the interaction of the support with a discontinuous rock mass. The

* *CSIR, Division of Mining Technology, P.O. Box 91230, Auckland Park, 2006.*

† *Colorado School of Mines, Golden, Colorado 80401-1887, United States of America.*

 SA ISSN 0038–223X/3.00 + 0.00. Paper received May. 1999; revised paper received Sep. 2000.

aim is to develop a more appropriate support design methodology. This approach to design should, within its own limitations, maximize support spacing, whilst maintaining a stable hangingwall span between support units. The methodology addresses hangingwall stability problems due to both quasi-static (rockfalls) and dynamic (rockbursts) failures. Due to widely varying rock mass conditions and behaviour of the reefs extracted by the gold and platinum mines, the methodology is influenced by local geological conditions. During the design stage, local rock and discontinuity types, as well as their spacing and orientation, need to be taken into account.

The final outcome of this work is a proposed design tool for the gold and platinum mining industry to assist the rock mechanics engineer to improve support design. Emphasis is placed on the estimation of optimized support spacing and support performance requirements for static and dynamic conditions. These proposals are untried in practice. Thus they will have to be assessed and calibrated under realistic conditions. The authors hope that the rock engineers in the industry will produce sufficient feedback to facilitate the next advance towards an even better support system design method.

Classification of rock mass discontinuities

Mining induced and geological discontinuities influence the behaviour and deformation of the rock mass surrounding stopes. Hence, in order to gain an insight into the support–rock mass interaction, a better understanding of typical rock mass discontinuities is required. Investigations into fractures in intermediate and deep level gold mine stopes have revealed that two main types of mining induced stress fractures are present in the hangingwall (Adams *et al.*[1]):

- *Shear Fractures*: These fractures are associated with highly stressed rock, and thus are found in intermediate and deep level mines. It is estimated that the fractures initiate 6 to 8 m ahead of the advancing stope face and separate the rock into blocks of relatively intact material. They are oriented approximately parallel to the stope face and are regularly spaced at intervals of 1 to 3 m. Shear fractures usually occur in conjugate pairs in the hangingwall and footwall, and typically reveal distinct signs of shear movement. Their dip in the hangingwall is generally towards the back area at angles of 60 to 70 degrees (Jager[2]; Esterhuizen[3]).
- *Extension Fractures*: These fractures initiate ahead of the stope face and are smaller than shear fractures. They form after shear fractures have propagated and generally terminate at parting planes. Extension fractures normally do not exhibit relative movement parallel to the fracture surface and are typically oriented parallel to the stope face. They are commonly spaced at intervals of 10 cm with lower and upper limits of 5 to 50 cm, respectively. The strike length is typically 3 m, where lower and upper limits of 0.4 and 6 m have been observed (Esterhuizen[3]). Extension fractures normally dip between 60 and 90 degrees, where the direction of dip (i.e. towards or away from the stope face) can be influenced by the hanging- and footwall rock types (Roberts[4]).
- Most gold reef extraction takes place in bedded quartzites. Bedding planes, which are parallel with the reef, often represent weak interfaces between adjacent strata, and provide little cohesion and low frictional resistance (Jager[2]). Bedding planes are generally spaced at 0.2 to 2.0 m intervals. The rock fall-out height is commonly governed by the position of bedding planes.

The three most prevalent discontinuity types, extension fractures, shear fractures and bedding planes, are illustrated in Figure 1. Their influence on the rock mass behaviour and stability is considered in this study. An attempt is also made to quantify their effect on support spacing and rock mass stability in static and dynamic conditions.

Numerical simulations of support interaction with a discontinuous rock mass

The finite-discrete element program ELFEN (Rockfield[5]) was used as a tool to investigate the interaction of support units with a discontinuous rock mass. Various ELFEN models were constructed, incorporating several discontinuity types. The aim of the numerical models was to gain a qualitative insight into the development of stress trajectories that arise from the load transmission between the support elements and the discontinuous hangingwall rock.

In the ELFEN models a beam, which was discretized by closely spaced extension fractures, simulated the fractured hangingwall. In intermediate and deep level mines, the extension fractures are typically oriented face parallel, where the fracture length in the dip direction is generally much longer than the fracture spacing in the strike direction. Hence, it is considered reasonable to model a section of the hangingwall along the strike direction in two dimensions, and assume plane strain conditions in the out-of-plane (dip) direction. The fracture surfaces were modelled with no cohesion and a friction angle of 40 degrees.

Along the top of the numerical models a uniformly distributed load was applied. In reality the hangingwall beam is probably not loaded uniformly. Local bed separations, as well as the influence of the unmined face and the extracted back area, can lead to irregular hangingwall loading. However, the aim of these simulations is to gain a qualitative view of the stress distribution within a discontinuous hangingwall beam. In these circumstances a simplification of the applied boundary conditions seems permissible.

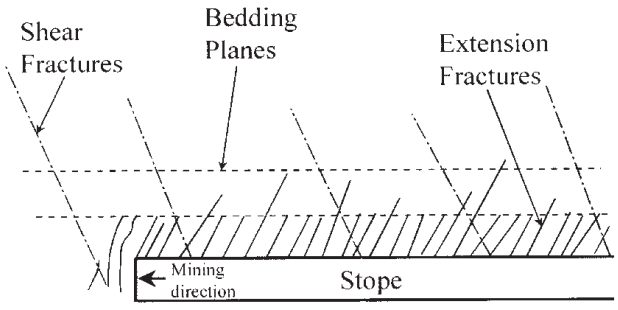

Figure 1—Simplified schematic illustrating the three most prevalent discontinuity types in intermediate and deep level mines

The hangingwall is assumed to be confined at both ends, i.e. at both the face and back area. Furthermore, the presence of a compressive horizontal stress is postulated in the beam. The effects of hangingwall confinement and of the compressive hangingwall stresses are significant and will be further discussed in the next section.

Figure 2 depicts the principal stress distribution induced by two prop-like support elements, when loaded by a hangingwall slab discretized into blocks by closely spaced vertical fractures. It is evident that the stresses are transmitted from the support units, through the long axis of the blocks defined by the vertical discontinuities, into the more competent (in this case not fractured) medium above the bedding plane.

In the case of a hangingwall beam discretized by dipping extension fractures and in the presence of a discontinuity modelling a shear fracture, the stress trajectories follow the paths shown in Figure 3. The stresses seem to be transmitted again mainly parallel to the discontinuities, through the fractured layer into the competent layer above the bedding plane.

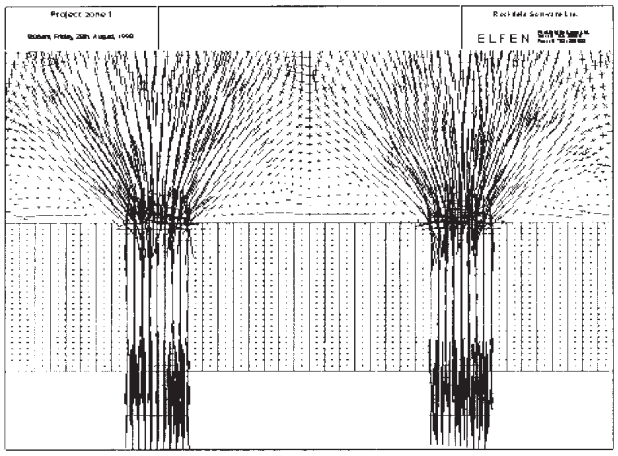

Figure 2—Stress distribution associated with a discontinuous hangingwall interacting with two support units

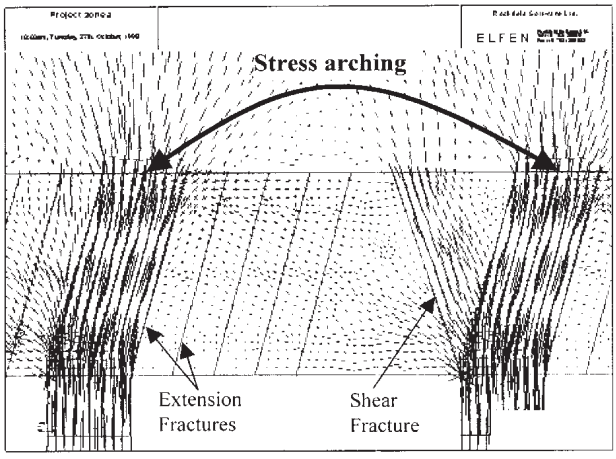

Figure 3—Stress transfer through a hangingwall beam discretized by discontinuities modelling extension and shear fractures

It is important to note that in Figures 2 and 3 those blocks of the discretized beam that are not directly supported are kept in position by friction. Furthermore, friction will be sustained only in the presence of horizontal normal stress. Thus, it is important to understand how the horizontal normal stress is induced and maintained in the hangingwall. In intermediate and deep mines, fracturing ahead of the stope face induces rock dilation, leading to compressive hangingwall stresses parallel to the skin of the excavation (Jager and Roberts[6]). The compressive stresses can be maintained only if the hangingwall beam is prevented from freely moving in the horizontal direction. The face obviously provides such a restraint. The situation at the end towards the mined-out area, however, requires further attention and is dealt with in the next section.

Compressive hangingwall stresses usually contribute significantly to the rock mass stability. Figure 4 shows the stress distribution associated with a model loaded in the vertical and horizontal direction. The magnitude of the horizontal stress is 1 MPa, whilst the total load carried by each support unit is 200 kN. These magnitudes are typical of values measured underground (Squelch[7]; Herrmann[8]). The stress distribution is complicated further by the addition of the horizontal stresses. It should be remembered, however, that the resultant stress field arises from the superposition of components due to the vertical and horizontal loads. Stress arching can be discerned in the competent layer (see Figure 4), leading to the conclusion that most of the forces transmitted by the support units follow a path parallel to the discontinuities, as observed in Figure 3.

To summarize, simplified numerical models representing a discontinuous hangingwall beam, discretized by extension fractures, a shear fracture and a bedding plane, have shown that the load carried by support units is generally transmitted in a direction parallel to the fracture orientations. Comparatively little stress is transmitted across the fractures, and the hangingwall rock between adjacent support units is essentially unstressed. When the hangingwall is clamped by compressive stresses acting parallel to the excavation surface, the resulting stress field can be approximated by the superposition of stresses due to horizontal and vertical loads. The majority of the stress induced by the support units continues to be transmitted parallel to the fracture surfaces.

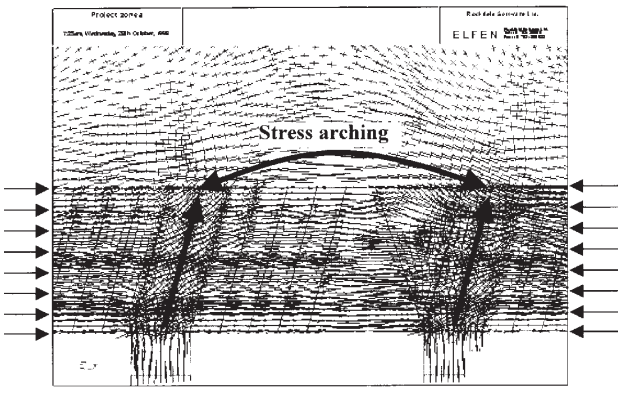

Figure 4—Vertical and horizontal loading of a discontinuous hangingwall beam

Hence, in results given in the following sections, the compressive stresses induced by support units are assumed to be transmitted parallel to the fracture surfaces. Support units do not directly stress the hangingwall rock between adjacent support units. Hangingwall stability in this region is governed by compressive stresses due to dilation and the buckling potential of the hangingwall beam.

Hangingwall confinement

An assumption implicit in this work is that the hangingwall rock is confined. Squelch[7] measured maximum compressive hangingwall stresses of 1 to 10 MPa at depths between 0.7 to 2.2 m into the hangingwall. These horizontal stresses clamp the fractured rock together and, depending on the orientation of the fractures, can significantly improve the structural integrity and stability of the hangingwall (Jager and Roberts[6]).

Herrmann[8] found that in stopes with back area caving, stress relaxation occurred in the lower layers of the hangingwall, and noted the importance of rock confinement to maintain compressive hangingwall stresses. Rockfalls and caving in the back area generally lead to reduced hangingwall confinement. However, compressive hangingwall stresses can still be maintained when frictional resistance generated at bedding planes restricts the lateral hangingwall movement. Such frictional resistance can be induced by appropriate support forces generated under the hangingwall beam, at or near to its end closest to the extracted area.

As an example of this mechanism, consider the stope shown in Figure 5. The elongates and packs shown here are assumed to be carrying a load of 200 kN and 400 kN, respectively. Thus, in order to estimate the horizontal compressive stress which can be maintained between the face and the two rows of elongates, the total load carried by the second elongate and the two packs is determined as 200 kN + 400 kN + 400 kN = 1000 kN. The self-weight of the rock between the second elongate and the packs is 160 kN (assuming a centre to centre support spacing of 3 m and a bedding height of 1 m). Thus the effective clamping force pinning the hangingwall to the bedding plane is 1000 kN–160 kN = 840 kN. If the bedding plane has an apparent friction angle of 40°, the maximum horizontal force which can be maintained is: (tan 40°) × 840 kN ≈ 700 kN, or, converting to stress, 0.7 MPa. Thus it is shown that, even with caving and rockfalls in the back area, reasonably high compressive hangingwall stresses can be maintained.

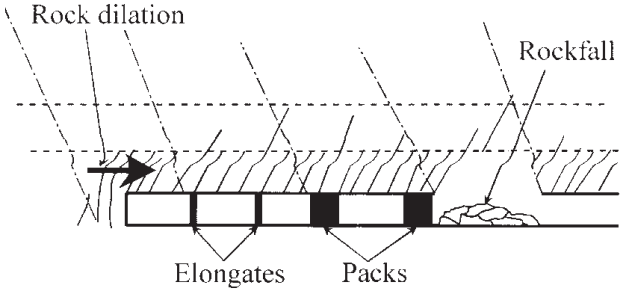

Figure 5—Stope with a back area rockfall leading to reduced hangingwall confinement

Quantifying stable hangingwall spans between support units

The qualitative insights gained from the numerical simulations are used to develop a simplified conceptual model describing the rock mass stability and quantifying stable spans between adjacent support units. It is believed that the model is suitable to incorporate into a support design procedure, which intends to optimize support spacing, while maintaining an acceptable level of safety. Details of the procedure of the proposed support design methodology are given in subsequent sections for rockfall and rockburst cases.

Two failure mechanisms are considered, namely instabilities due to (i) beam buckling and (ii) shear failure due to slip at the abutments.

Hangingwall beam buckling

The design procedure followed here is based on that developed by Evans[9], and subsequently modified and extended by Beer and Meek[10], Brady and Brown[11], and Hutchinson and Diederichs[12]. The solution technique, which is based on the voussoir beam, follows the intuitive idea that, in a discontinuous hangingwall beam, the central transverse crack determines the deformational behaviour (Figure 6). In the buckling mode the beam becomes unstable to form a 'snap-through' mechanism.

In analysing the stability of the voussoir beam the following assumptions are made:

- As the beam deflects, a parabolic compression arch develops in the beam
- Deflection of the beam occurs before slippage at the abutments. Stability against slippage (see next section) is determined after the compression arch develops
- The abutments are stiff, i.e. they do not deform under the arching stress. Each abutment is subjected to the same distributed load as the ends of the beam, however the loaded area is small compared with the beam span. Therefore, elastic compression of the abutments will be small compared with the beam compression, and may be neglected (Brady and Brown[11]).

The voussoir beam problem is statically indeterminate, i.e. no explicit solution is available and an iterative process is

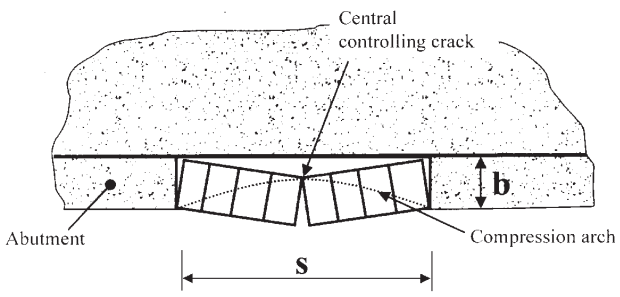

Figure 6—Voussoir beam geometry for hangingwall beam analysis

followed to determine the beam equilibrium position. The solution procedure is given in texts such as Brady and Brown[11], and Hutchinson and Diederichs[12], and is not repeated here.

Previously documented results of this solution have used an absolute snap-through limit, which is the limit of stable deflection according to the mathematical formulation. This limit is extremely sensitive to beam thickness, a difficult parameter to estimate accurately and reliably. Hutchinson and Diederichs[12] recommend a design snap-through limit which is reached when the mid-span deflections reach 10 per cent of the beam thickness. Beyond this deflection, small differences in thickness have an unacceptably large influence on stability, and the beam's stability becomes uncertain.

Using the design snap-through limit of Hutchinson and Diederichs[12], the span versus minimum beam thickness is given in Figure 7. The snap-through limits are given for various values of *in situ* rock mass elasticity modulus (E`) parallel to the excavation surface. The *in situ* rock mass modulus is predominantly governed by the stiffness of the rock mass discontinuities, and is lower than the stiffness of solid rock, which is characterized by the Young's modulus. It is apparent from Figure 7 that the relationship between span and beam thickness is highly dependent on the *in situ* rock mass modulus measured in a direction parallel to the excavation surface.

Bandis *et al.*[13] made use of experimental data to establish a relationship between normal joint stiffness and normal stress for well interlocked joints in various rock types (Figure 8). The joint stiffness is found to increase with increasing normal stress. For rock mass discontinuities in a typical gold or platinum hangingwall, where the compressive hangingwall stresses are generally less than 5 MPa, a discontinuity stiffness of 40 MPa/mm is assumed for the purposes of this study. It is recognized, however, that further *in situ* discontinuity stiffness measurements are required to obtain more accurate and representative stiffness data.

The joint stiffness is incorporated in the buckling analysis procedure. To simplify the analysis, and in view of the comparatively minor variations in stiffness for normal stresses ranging from 0 to 5 MPa, the stiffness is assumed to be constant. The value selected was 40 MPa/mm, irrespective of the compressive stresses acting within the hangingwall beam.

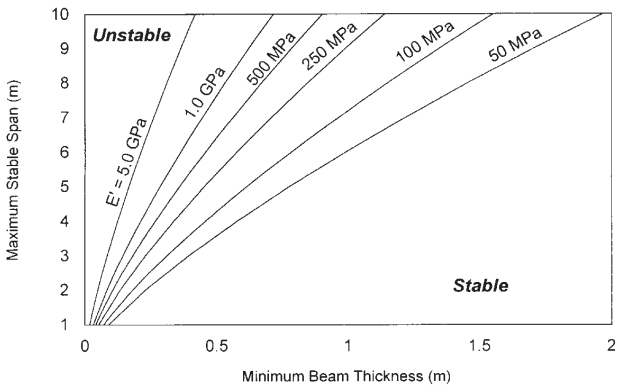

Figure 7—Span versus minimum beam thickness at 10% beam deflection for various values of *in situ* rock mass modulus (E`)

The effective rock modulus (E`) is calculated by multiplying the normal joint stiffness by the lateral deformation (arch shortening) during beam deflection. It is thus assumed that lateral hangingwall deformation occurs at the discontinuities only, and the rock between adjacent discontinuities does not deform. This is a realistic assumption as the Young's modulus of the intact rock is much higher than the effective joint modulus.

Multiple discontinuities act as springs in series, and each discontinuity is compressed equally. Span versus thickness relations shown in Figure 9 give the stability envelopes of hangingwall beams with 3 joints, as well as 1, 3, 5 and 10 joints per metre of hangingwall length. As shown in Figure 6, the unsupported hangingwall span needs to be discretized by at least 3 joints to allow deformation in the buckling mode. Hence, the line shown in the graph of Figure 9 indicating the stability envelope of a hangingwall discretized by 1 joint per metre is only shown for maximum stable spans exceeding 3 metres. At spans below 3 metres the beam would be discretized by less than 3 joints, and thus no deformation in the buckling mode would be possible.

As the beam deflects, the arch stresses are transmitted through the beam edges to the abutments. The maximum abutment stresses for various beam thicknesses are plotted in Figure 10 as a function of span (postulating 5 joints per metre). It is evident that the maximum abutment stress for typical beam thicknesses encountered in South African mines

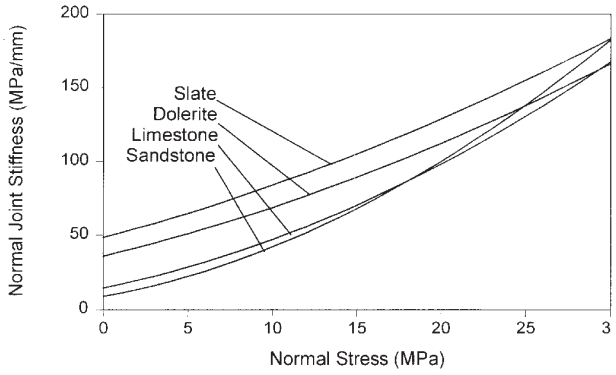

Figure 8—Normal joint stiffness for well interlocked joint examples in various rock types (after Bandis *et al.*[13])

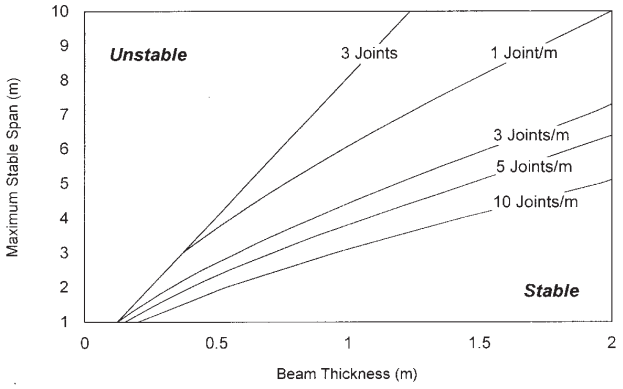

Figure 9—Buckling stability envelopes of a discontinuous hangingwall beam

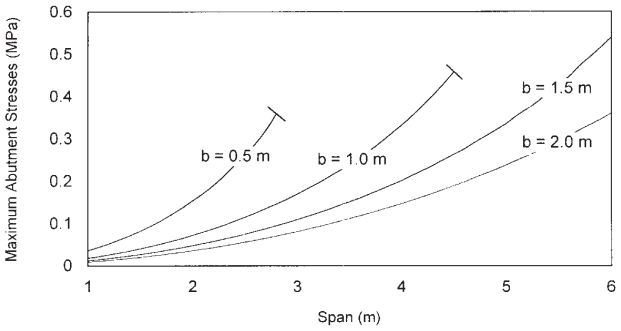

Figure 10—Maximum abutment stresses versus span for various beam thicknesses

is approximately 0.4–0.5 MPa for spans ranging from 2.5 to 6 m. However, these are localized stresses induced by block rotation. If these stresses are averaged across the full thickness, the mean compressive stress in the buckling mode is considerably lower than the earlier calculated magnitude.

Shear and rotational failure by slip at the abutments

The second failure mechanism considered in this study is shear and rotational failure by slip at the abutments. In Figure 11 a schematic diagram is depicted of the geometry governing the stability of a hangingwall keyblock. Here shear forces prevent the fall of the block. To analyse this situation in some detail, the following notations are introduced. The weight of the block is denoted by W, the beam thickness by b, the span between adjacent support units by s and σ_x is the magnitude of compressive horizontal stress in the hangingwall. Finally, α and β are the angles that define the orientation of the extension and shear fractures. The hangingwall stress may be generated by two mechanisms, namely:

- In intermediate and deep level mines, the rock dilation associated with fracturing immediately ahead of the stope face may induce compressive stresses parallel to the excavation surface
- The block rotation associated with the 'snap-through' failure mechanisms described previously may also generate compressive stresses in the hangingwall.

The discontinuities, which represent mining induced fractures, are assumed to have zero cohesion on the inclined contact surfaces. Hence, for the keyblock to be stable, the lateral thrust at the abutments due to *in situ* compressive hangingwall stresses must mobilize a frictional resistance sufficient to provide the abutment shear force. The frictional resistance for either side of the keyblock can be calculated using the following expressions:

$$V_I = -\sigma_x b \cot(\alpha + \varphi) \text{ and } V_{II} = -\sigma_x b \cot(\beta + \varphi) \qquad [1]$$

The coefficient of friction, μ, is an important parameter governing the resistance to shear and it defines the angle of friction $\varphi = \arctan(\mu)$. Typically, underground discontinuities have closely matched surfaces, especially in the case of mining induced fractures. Hence, the apparent friction angle can be relatively high; a range of 30 to 50 degrees is considered realistic.

Stability or instability of the keyblock depends on various factors. The criteria for stability are summarized as follows:

- *Unconditional stability*. The keyblock is unconditionally stable (Figure 12a) if the forces and moments are both in equilibrium. The forces will not induce the fall of the block if $V_I + V_{II} > W$. Similarly, the moments will not cause dislodging movements (rotation) if the supporting forces satisfy the following inequalities: $V_I > 1/2\ W$ and $V_{II} > 1/2\ W$. Obviously, if the two conditions concerning moments are satisfied, the first criterion will also be fulfilled. A set of necessary and sufficient criteria for unconditional stability can be found from the relationships in Equation [1] in terms of the angles. The conditions for unconditional stability can now be expressed as follows:

$$\alpha > \frac{1}{2}\pi - \varphi \text{ and } \beta > \frac{1}{2}\pi - \varphi \qquad [2]$$

- *Conditional stability*. If only the criterion concerning forces and *one* of those arising from moments are satisfied, then the block may or may not be stable. To illustrate such a situation, postulate the following:

$$V_I + V_{II} > W; \quad V_I < \frac{1}{2}W; \quad V_{II} > \frac{1}{2}W \qquad [3]$$

Clearly this block is not unconditionally stable, but it may *not* become dislodged if its rotation is *kinematically impossible*. Such a case is illustrated in Figure 12c. If, however, rotation is possible, failure will occur and the block will fall (Figure 12d).

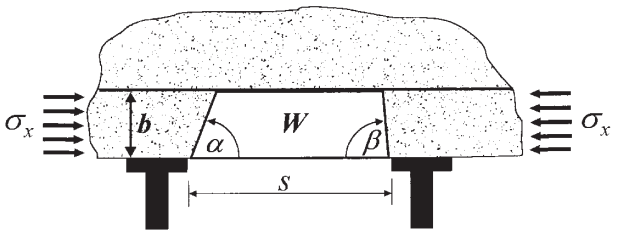

Figure 11—Potential keyblock instability due to shear failure at the abutments

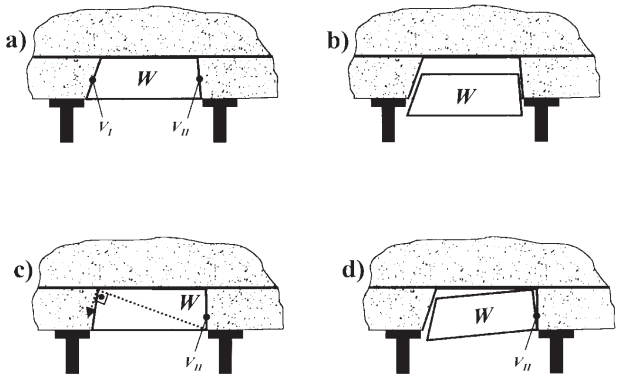

Figure 12:—Schematic diagrams showing possible failure modes due to shear at discontinuity interfaces: a) Keyblock is stable as $V_I > 1/2\ W$ and $V_{II} > 1/2\ W$. b) Keyblock shear failure as $V_I < 1/2\ W$ and $V_{II} < 1/2\ W$. c) Although $V_I < 1/2\ W$, the keyblock is stable as $V_{II} > 1/2\ W$ and no block rotation is possible. d) Keyblock is unstable as $V_I < 1/2\ W$ and block rotation is kinematically possible ($V_{II} > 1/2\ W$)

The next task is to determine the criteria that prevent rotation. As an example, postulate that the block, if it moves, will pivot around its furthermost hangingwall point on the left (see Figure 13). Let this point of fulcrum be *A*. Denote by *r* the distance between the fulcrum and point *B*, the furthest point on the right of the top plane of the block. Rotation can occur only if point *B* can move past the next block to the right.

Let *C* be the point where the fracture at the right end of the block intersects the hangingwall. Clearly, the limiting geometry is when the block can start to pivot around its fulcrum, that is, around point *A*. This can occur when the line $\overline{BC}$ (in section) is tangent to the circle of radius *r* with its centre at point *A*. If we denote the angle enclosed by lines $\overline{AC}$ and $\overline{AB}$ by ε, then this criterion is satisfied if $\varepsilon + \beta = 1/2\ \pi$. Thus if $\varepsilon + \beta \leq 1/2\ \pi$, the keyblock can rotate around its fulcrum and, if $\varepsilon + \beta > 1/2\ \pi$, keyblock rotation is kinematically impossible.

Now introduce the ratio $\kappa = b/s$. It is simple to show that

$$\varepsilon = \arctan\left(\frac{\kappa}{1-\kappa\cot(\beta)}\right). \quad [4]$$

These two relationships are sufficient to obtain the following results:

$$\kappa(\beta) = \frac{1}{2}\sin(2\beta) \text{ or alternatively } \beta(\kappa) = \frac{1}{2}\arcsin(2\kappa). \quad [5]$$

The first of these relationships is depicted graphically in Figure 14. In this illustration, rotation is prevented for cases that fall above the curve, therefore, the block is *stable*. In instances that plot on or under the curve rotation can occur, and hence the block is *unstable*. Since the value of the sine function does not exceed unity, it is obvious from the first of these expressions that instability cannot occur when $\kappa > 1/2$ or $b > 1/2\ s$. It is evident from Figure 18 that $\kappa(\beta)$ is a double valued function. If we denote the two solutions by β_1 and β_2 ($0 < \beta_1 \leq 1/4\ \pi$ and $1/4\ \pi \leq \beta_2 \leq 1/2\ \pi$), the stability conditions concerning the block can be summarized as follows:

Stable: a) If $\kappa \leq 1/2$ and $\beta < \beta_1$ or $\beta > \beta_2$
b) If $\kappa > 1/2$

Unstable: If $\kappa \leq 1/2$ and $\beta_1 \leq \beta \leq \beta_2$.

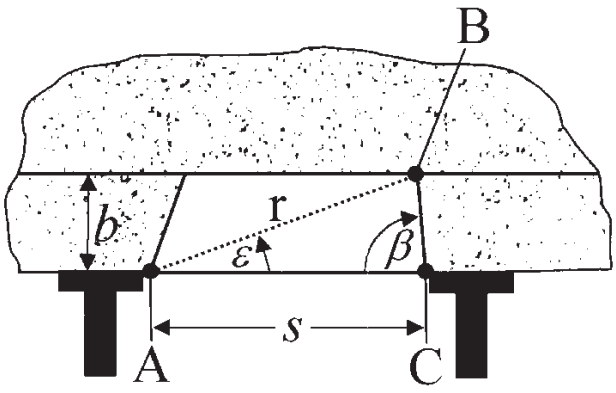

Figure 13—Geometry parameters governing the rotational stability of hangingwall blocks

It is obvious from Figure 15 that the upper bound of the span that will not rotate increases (for a fixed beam thickness) as the value of angle β (or α) departs, up or down, from 45 degrees. It is also noteworthy that for situations where *b* is greater than 2 m, rotation is unlikely to limit the stability of the hangingwall.

The above discussion is valid for keyblocks having a geometry as shown in Figure 13. For certain keyblocks delineated by shallow dipping discontinuities and/or small spans, however, the geometry could be of the form shown in Figure 16. In this case keyblock rotation is kinematically impossible if $\alpha + \beta > 1/2\ \pi$.

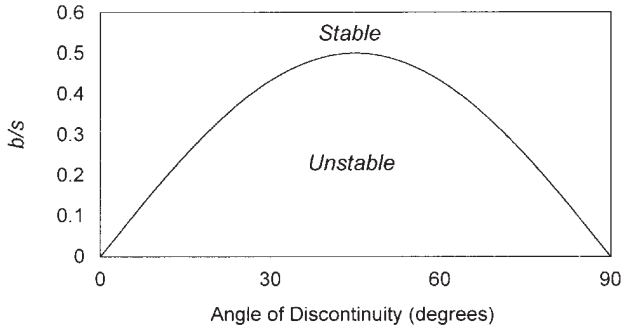

Figure 14—Stability envelopes characterized by the ratio of *b* over *s* versus discontinuity angle

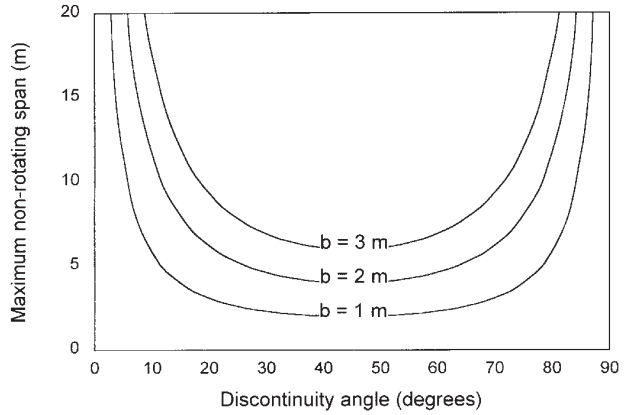

Figure 15—Upper limit of stable spans

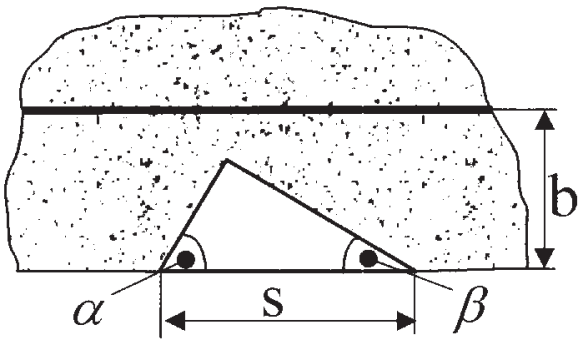

Figure 16—Keyblock geometry delineated by shallow dipping discontinuities and/or small spans

An interesting particular case occurs when all fractures are parallel. Postulate that the face is on the left-hand side. In this case $\alpha = \pi - \beta$ and the expression for the vertical component of the shear resistance on the left becomes:

$$V_I = \sigma_x b \cot(\beta - \varphi) \quad [6]$$

(note the change in sign) and the formula for V_{II} remains unaltered. This expression remains positive as long as

$$\varphi < \beta < \frac{1}{2}\pi + \varphi \quad [7]$$

It is obvious from these expressions that $V_I > V_{II}$ as long as $\beta > \varphi$. Since this criterion is almost always satisfied in practice, it can be concluded that this block is unconditionally stable in most cases, provided $V_{II} > {}^1/_2\, W$.

Rockfall support design methodology

In the hope of progressing beyond the current state of stope support design, methodologies are proposed to assess the suitability of a particular support system. Supports to prevent quasi-static failure (rockfall) and dynamic collapse (rockburst) are to be treated separately. In this section the rockfall case is discussed and the next section deals with the dynamic case. The procedures put forward are tentative and will have to be tested in the field.

Load bearing requirements and support spacing are assessed for a given support system with a view to preventing rockfalls. The support system evaluation consists of two phases, namely:

- The already familiar tributary area theory is applied to determine if the load bearing requirements of the support system are met
- The support spacing and stability of spans between adjacent support units are checked by investigating the possibility of failure due to the two predominant failure mechanisms outlined in the previously two sections, that is, (i) beam buckling, or (ii) shear failure due to slip at the abutments.

The following assumptions are made in the course of the evaluation.

- The position of prominent bedding planes and/or back analyses of previous rockfall accidents determine the rock mass fall-out thickness. Work by Roberts[4], which was recently updated by Daehnke *et al.*[14], has shown that the fall-out thickness is reef dependent and is equal to 1.0 m for the Carbon Leader Reef, and 1.2 m for the Vaal Reef and Ventersdorp Contact Reef.
- The hangingwall rock mass is discretized by face parallel extension and shear fractures. At this stage no attempt has been made to include discontinuities of geological origin; unlike mining induced fractures, these are generally not face parallel and need to be considered in future work.
- The load bearing requirements, due to tributary area load distributions, are calculated on the basis of a plan of the stope showing the proposed support system (Figure 17a).
- Maximum stable spans are calculated to prevent hangingwall collapse due to buckling or shear failure. The cross-section of the stope region is taken along the strike direction, that is, perpendicular to the face (Figure 17b).

The solution procedure can be coded readily to facilitate the rapid and convenient evaluation of various support systems and associated spacing of support units. Figure 18 depicts a flow chart of the discussed method.

The parameters governing the maximum stable hangingwall span are the discontinuity angles (α and β), the fall-out height (b), the friction coefficient (μ), and the hangingwall clamping stress (σ_x). The influence of these parameters on the stable span is investigated next.

The maximum span was determined using the proposed rockfall design methodology for a mine in intermediate depth with 5 fractures per metre in the hangingwall. Possible failures due to buckling and slip at the discontinuities are analysed. The limiting equilibrium of the keyblock is governed by one of two failure mechanisms: (i) shear failure due to slip at the abutments and/or block rotation, and (ii) buckling failure. Figure 19 gives stability envelopes for the hangingwall at limiting equilibrium for σ_x = 1.0 MPa, b = 1.0 m and μ = tan 40°.

As is evident from Figure 19, the maximum stable span for the case study investigated here varies from zero to 3.8 m. The maximum span is governed by three types of failure mechanisms, which depend on the combinations of discontinuity angles (α and β). A set of stability definitions in the various parts of the α, β plane are illustrated in Figure 21. The plane is subdivided into four regions and these regions are delineated by inequalities.

Region A: This region is defined by $0 < \alpha \leq \alpha_{min}$ and $0 < \beta \leq \beta_{min}$, where $\alpha_{min} = \beta_{min} = {}^1/_2\, \pi - \varphi$, as defined previously in Equation [2]. Hence, for the example given here ($\varphi = 40°$),

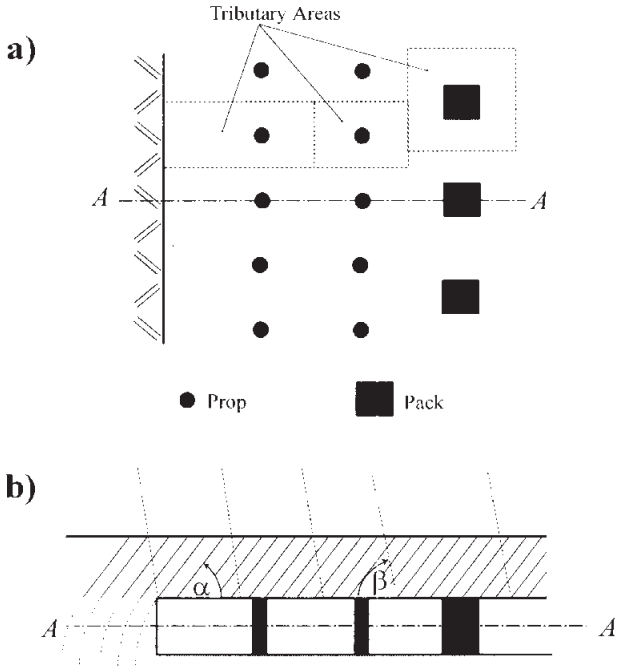

Figure 17—a) Plan view applied for tributary area load requirements (top), and b) face perpendicular cross-section used to determine maximum stable hangingwall spans in strike direction

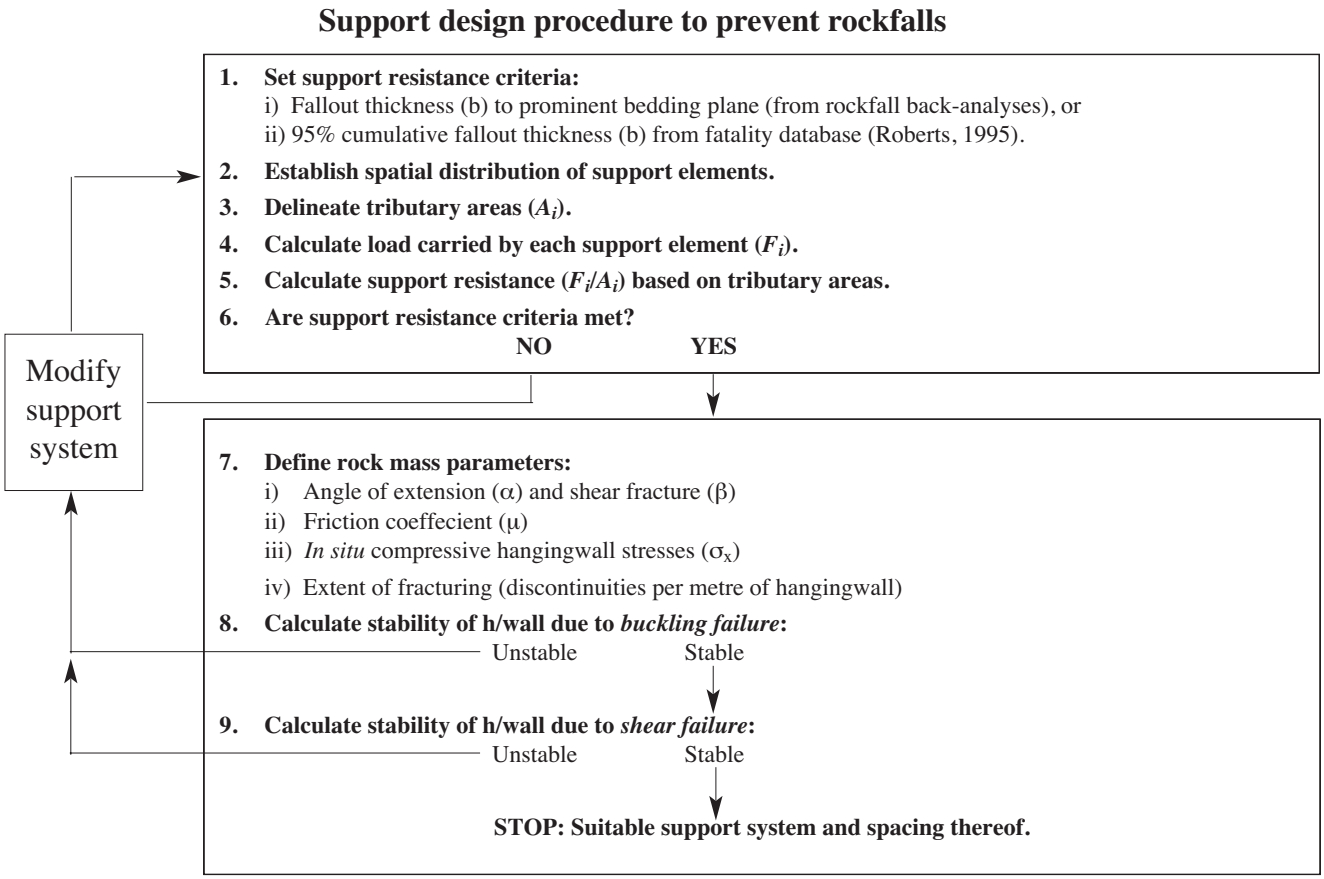

Figure 18—Flow chart showing methodology of the evaluation of stope supports proposed to prevent rockfalls

$\alpha_{min} = \beta_{min} = 50°$. At angles $0 < \alpha \leq \alpha_{min}$ and $0 < \beta \leq \beta_{min}$ the supporting forces V_I and V_{II} are negative, and hence all keyblocks, irrespective of size, are *unstable*. This is evident from Figure 19, and for $0 < \alpha \leq \alpha_{min}$ and $0 < \beta \leq \beta_{min}$ the maximum stable span is zero.

Region B: Here the limits are defined by $\alpha_{min} < \alpha \leq 1/2\ \pi$ and $0 < \beta \leq \beta_{min}$. Thus $V_I \geq 0$, $V_{II} < 0$ and the keyblock is conditionally stable, depending on whether keyblock rotation is kinematically possible. In the previous section it was shown that it is kinematically impossible for a keyblock to rotate if $b/s \geq 1/2 \sin(2\beta)$. This condition holds for keyblocks having the shape shown in Figure 20a. For keyblocks with a short span (Figure 20b) the stability condition to prevent rotation becomes $\alpha + \beta > 1/2\ \pi$. Hence, in Region B, keyblocks rotate and are unstable if $\alpha + \beta \leq 1/2\ \pi$ (see Figures 19 and 21). The maximum stable span at $\alpha + \beta = 1/2\ \pi$ corresponds to a keyblock having the shape shown in Figure 20c.

Region C: Here the boundaries are given by the following inequalities $0 < \alpha \leq \alpha_{min}$ and $\beta_{min} < \beta \leq 1/2\ \pi$. For these angles $V_I < 0$, $V_{II} \geq 0$ and the keyblock is conditionally stable, depending on whether rotation is kinematically possible. The conditions outlined for Region B are also applicable to Region C, and are thus not repeated here.

Region D: This region is delineated by $\alpha_{min} < \alpha \leq 1/2\ \pi$ and $\beta_{min} < \beta \leq 1/2\ \pi$. Here $V_I \geq 0$, $V_{II} \geq 0$ and comparatively large spans are stable. The upper limit of the stable spans are governed by the buckling potential of the beam. Figure 9 gives the maximum stable spans versus beam thickness for a hangingwall discretized by various numbers of joints. For the case study shown in Figure 19 ($b = 1$ m, 5 Joints/m), the maximum stable span governed by the buckling potential is 3.8 m.

Figure 22 shows the influence of hangingwall beam thickness (b) on the maximum stable span at limiting equilibrium for various angles of discontinuities. It is apparent that the maximum stable span decreases with decreasing beam thickness.

The effect of compressive hangingwall stresses on the maximum stable span is given in Figure 23. It is evident that reduced compressive stresses decrease the stability and associated stable span lengths between adjacent support units. In particular, as the compressive stresses are reduced from $\sigma_x = 0.1$ MPa to 0.01 MPa, the stable hangingwall span is considerably reduced from a maximum of 4 m ($\sigma_x = 0.1$ MPa) to 1 m ($\sigma_x = 0.01$ MPa). This stress is clearly a critical component and it requires further study.

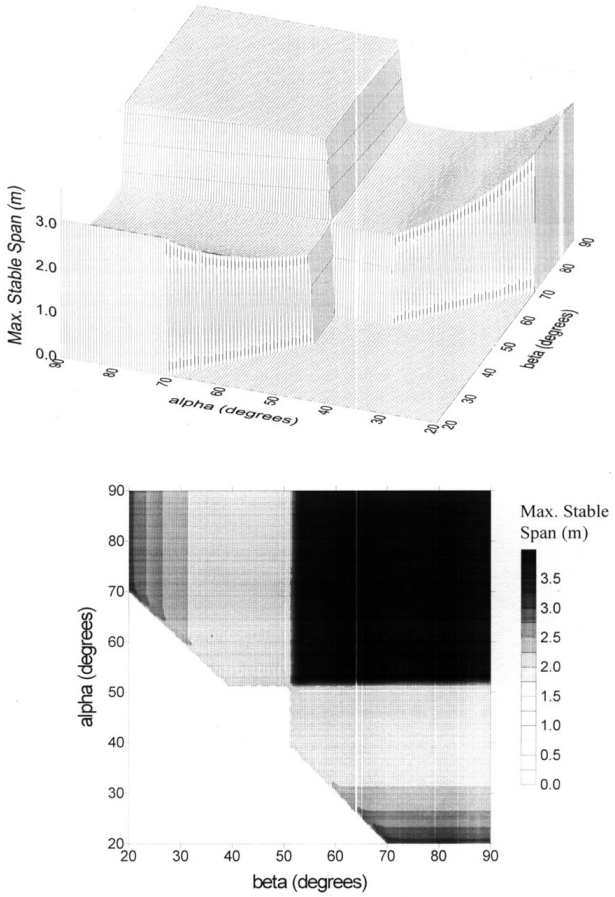

Figure 19— Maximum stable span versus discontinuity angles for σ_x = 1.0 MPa, *b* = 1.0 m and μ = tan 40°. Both carpet (top) and contour (bottom) plots are given to facilitate convenient data interpretation

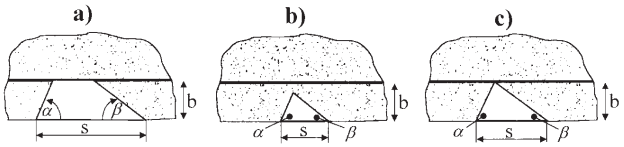

Figure 20— Various keyblock shapes associated with different rotational stability conditions

Figure 24 gives the effect of various coefficients of friction (μ) on maximum stable spans. As the coefficient of friction is decreased, the size of Region A is increased. This results in an increased possibility of shear failure and consequently for smooth rock mass discontinuities greater areal coverage requirements are necessary.

The methodology proposed here is likely to be better suited for comparatively densely fractured hangingwall, consisting of hard rock, as typically encountered in intermediate and deep level gold and platinum mines. The method is unlikely to be applicable to shallow mines, such as collieries, where the surrounding rocks are relatively soft. In these mines, due to sedimentation, often intensively laminated roof strata is encountered. The failure of such laminated roof are controlled by mechanisms not discussed in this paper.

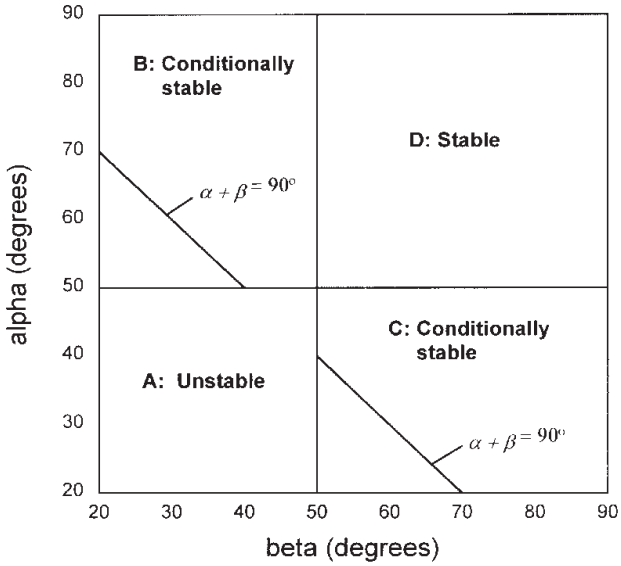

Figure 21—Stability definitions in the various parts of the α, β plane

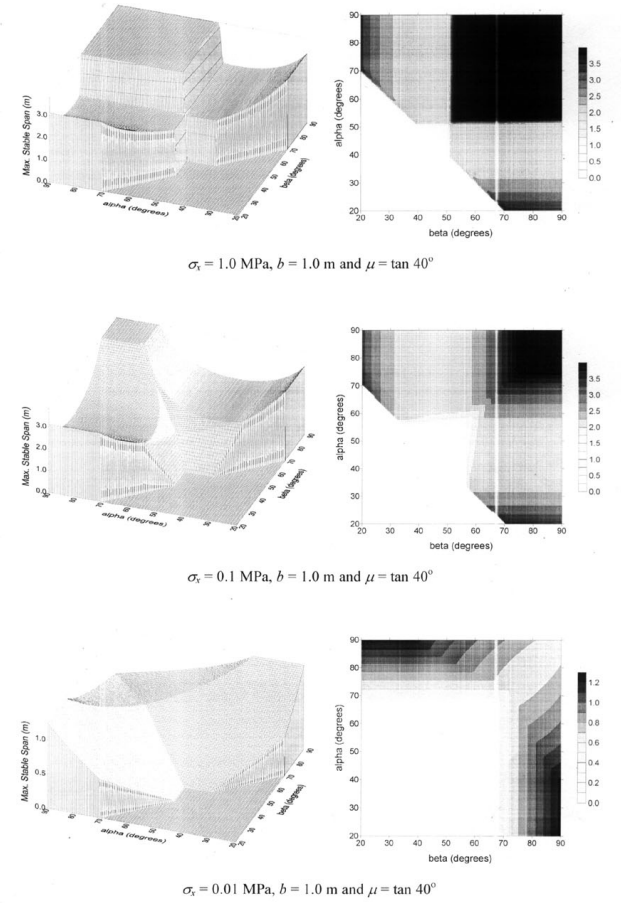

Figure 22—Effect of reduced hangingwall beam thickness (*b*)

Support design in the presence of rockbursts

In seismic and rockburst prone mines, sudden fault rupture or the explosive failure of highly strained rock leads to energy being radiated in the form of stress waves. The stress

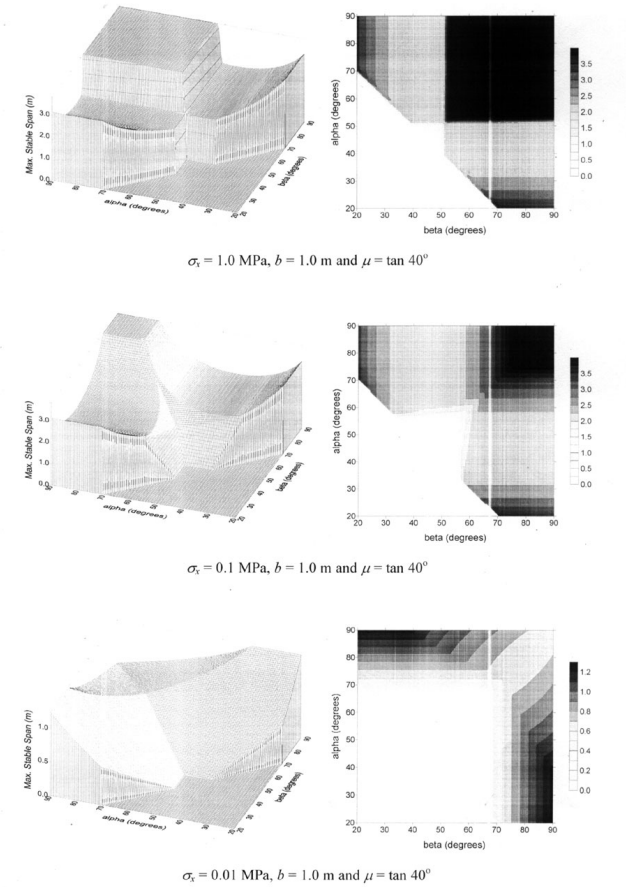

σ_x = 1.0 MPa, b = 1.0 m and μ = tan 40°

σ_x = 0.1 MPa, b = 1.0 m and μ = tan 40°

σ_x = 0.01 MPa, b = 1.0 m and μ = tan 40°

Figure 23— Effect of reduced hangingwall compressive stresses (σ_x)

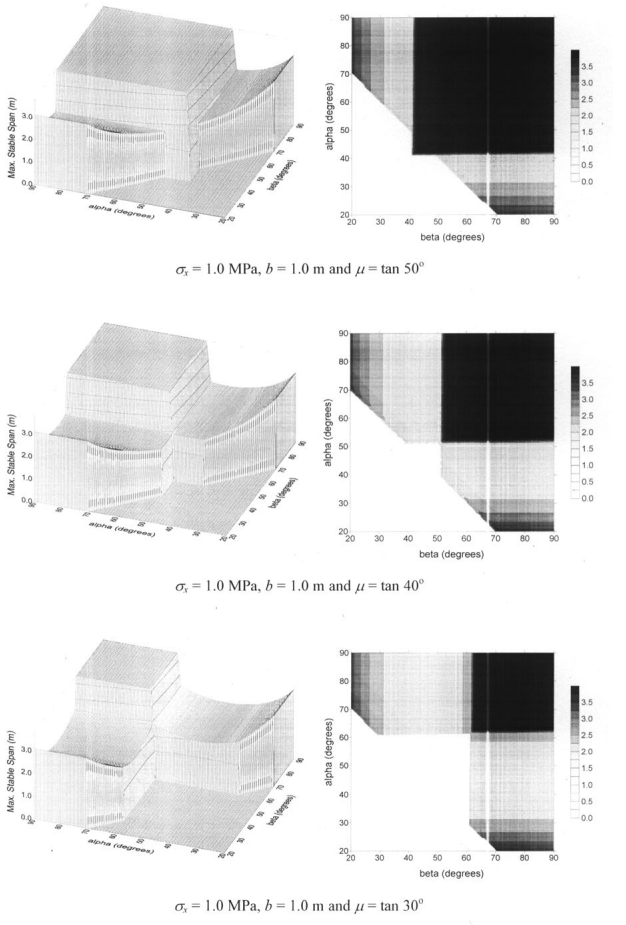

σ_x = 1.0 MPa, b = 1.0 m and μ = tan 50°

σ_x = 1.0 MPa, b = 1.0 m and μ = tan 40°

σ_x = 1.0 MPa, b = 1.0 m and μ = tan 30°

Figure 24— Effect of coefficient of friction (μ)

waves interact with mining excavations, leading to interface and surface waves, energy channelling and wave focusing (Kirsten and Stacey[15], Ortlepp[16], Daehnke[17]). The rock is subjected to rapid accelerations, resulting in rock fabric failure, keyblock ejection and stope closure. The most widely used support design criterion used in rockburst prone mines is based on work of Wagner[18], which takes into account the kinetic and potential energy of the keyblocks. Underground observations, rockburst back analyses and numerical simulations have indicated that hangingwall blocks can be accelerated to velocities of up to 3 m/s. The criteria for effective support systems are thus to absorb the kinetic and potential energy associated with the hangingwall moving with an initial velocity of 3 m/s. Roberts[4] assumed that during a rockburst the hangingwall must be brought to rest within 0.2 m of downward movement, i.e. the total energy which had to be absorbed by the support system is:

$$E = \frac{1}{2}mv^2 + mgh, \qquad [8]$$

where E is the total energy to be absorbed by the support system, m is the mass of the hangingwall (dependent on fall-out height), v is the initial hangingwall velocity (taken as 3 m/s) and h is the downward hangingwall displacement (taken as 0.2 m).

In the design methodology proposed here, the hangingwall is also assumed to have an initial velocity of 3 m/s, however the downward displacement (h) is determined from the energy absorption capabilities of the support units (Figure 25 and Equation [9]). Thus the total hangingwall displacement up to the point in time when motion ceases is greater for a support system providing less support resistance, while a high resistance support will arrest the hangingwall within a shorter distance. In the first case the hangingwall deceleration is reduced, however, the potential energy component, which needs to be absorbed by the support system, is increased. In the second case the hangingwall deceleration is higher and the potential energy component is decreased.

$$\int_{h_1}^{h_2} F(x)dx = \frac{1}{2}mv^2 + mgh, \text{ where } h = h_2 - h_1 \qquad [9]$$

To illustrate the load bearing requirements of a support unit during a dynamic event, assume a support unit with force deformation characteristics shown in Figure 26 is installed underground. Due to pre-stressing and stope convergence, the unit is quasi-statically deformed up to point h_1; thereafter a rockburst occurs and the unit is rapidly compressed to point h_2. The hashed area of the graph in Figure 26 defines the total energy, which is required to arrest the hangingwall. For the support system to meet the rockburst loading requirements, the following criteria apply.

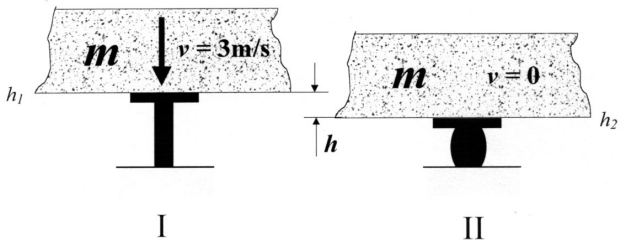

Figure 25—Conceptual model of dynamic hangingwall displacement and associated energy absorption requirements of the support system, where h_1 and h_2 is the closure acting on the support unit before and after the dynamic event, respectively

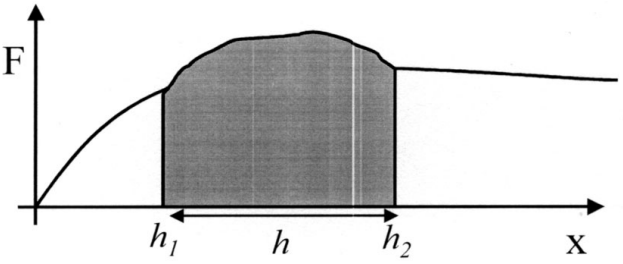

Figure 26—Quasi-static and dynamic force-deformation behaviour of a support unit prior and during a rockburst

- The average dynamic hangingwall displacement (h) in the stope should not exceed 0.3 m. If the mean displacement would exceed this value, differential downward movements between the face and the support units, as well as between different supports of varying stiffness, could compromise the post-rockburst hangingwall integrity. This would lead to a heavily fractured hangingwall with low structural strength. Further work needs to be done to provide a more appropriate estimate of h. However, in this preliminary study, a maximum value of $h = 0.3$ m is considered realistic and suitable for initial support design trials.
- To ensure post-rockburst stability, the load borne by each support unit after the rockburst, that is $F(h_2)$, should exceed the corresponding tributary load.
- The stoping width minus h_2 should exceed 0.7 m to ensure a sufficient post-rockburst stoping width to prevent injury to and allow movement of mine personnel.

Having calculated h using [9], the local hangingwall deceleration can be determined from the equations of motions (assuming linear deceleration from $v = 3$ m/s).

$$a = \frac{v^2}{2h} \qquad [10]$$

Taking the acceleration due to gravity into account, the *effective* hangingwall weight is calculated from the following relationship:

$$W_{eff} = m\left(g + \frac{v^2}{2h}\right) \qquad [11]$$

The procedure of designing rockburst resistant support follows similar lines to those presented as part of the methodology of evaluating stope support for the purposes of combating rockfalls. The assumptions made in the rockfall related case also hold in rockburst prone mines. The main difference between the two procedures is that in the rockburst related case the effective hangingwall weight in [11] replaces the static weight of $W = m\,g$. Figure 27 illustrates the salient features of the rockburst-proof support design.

The effect of dynamic hangingwall displacement (h) is shown in Figure 28. Reduced displacement implies higher hangingwall deceleration and associated higher effective weight. This affects the hangingwall stability primarily in the buckling mode, and reduced stable spans are evident.

Conclusions

A unified methodology to evaluate support systems catering for rockfall and rockburst conditions is proposed. The method consists of two stages: (i) a tributary area analysis determines the general support resistance requirements for the support system as a whole, and (ii) a stability analysis considering failure due to beam buckling and shear at the beam abutments gives maximum spacing of individual support units.

The methodology is particularly suited to mines in intermediate and great depth, where, typically, the hangingwall consists of hard rock and is highly discontinuous due to face parallel mining induced fractures.

The support design method gives insights into spacing and associated stable hangingwall spans in the strike direction only. Due to the face parallel mining induced fracture orientation in intermediate and deep level mines, the hangingwall rock is generally less prone to failure between two support units in the dip direction, compared to failure between units in the strike direction. Probabilistic keyblock analyses (Daehnke *et al.*[14]) have shown that, for a typical discontinuity spacing and attitude as encountered in intermediate depth and deep gold mines, the support spacing in the dip direction can be increased by a factor of ± 1.5 compared with the strike spacing, while maintaining an equal probability of keyblock failure in the dip versus strike direction. Hence, to propose a prudent system, it is recommended that the support spacing in the dip direction should not exceed 1.5 times the spacing in the strike direction.

It is recommended that additional work be conducted to quantify the effects of arbitrarily oriented discontinuities of geological origin on support spacing in the strike and dip directions. Further work could re-address the influence of the modified hangingwall stress distribution and zones of influence due to loading by the stope face, support units and backfill. The horizontal clamping stress is a vital part of the design procedure. Further work needs to be done to clarify the magnitude and role of this important component.

It should be remembered that the method proposed is untried in the field and, before its full acceptance, it should undergo field trials. Parametric evaluations of the proposed support design methodology show that, for typical discontinuities observed underground (i.e. dipping between 50° and 90°), the design procedure provides realistic spans

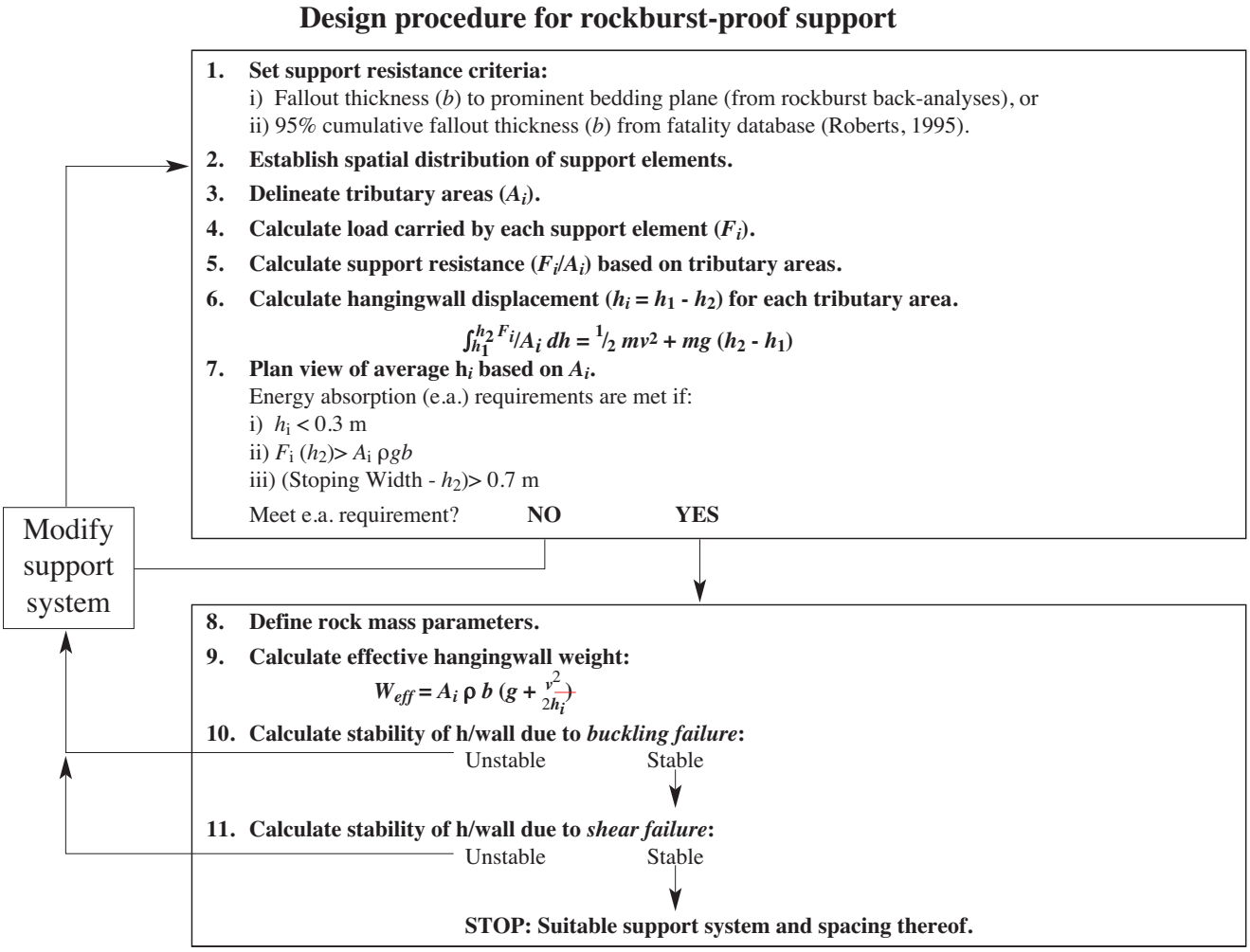

Figure 27—Flow chart showing features of the rockburst support design methodology

corresponding to typical spacing of support units in current gold and platinum mines.

Acknowledgements

This work forms part of the stope support research programme of Rock Engineering, CSIR Division of Mining Technology under SIMRAC Projects GAP 330, GAP 613 and GAP 627. The author acknowledges the financial assistance and support received from the Safety in Mines Research Advisory Committee (SIMRAC). The authors further wish to thank Dr T.O. Hagan, Mr A.J. Jager and Dr J.A.L. Napier for reviewing the manuscript and making useful comments and suggestions.

References

1. Adams, G.R., Jager, A.J., and Roering, C. Investigations of the rock fracture around deep-level gold mine stopes. *22nd U.S. Symposium on Rock Mechanics,* Massachusetts Inst. of Technology, June 28–July 2. 1981.
2. Jager, A.J. Personal communication on the structure of discontinuous hangingwalls in deep level mines. CSIR: Division of Mining Technology, Carlow Road, Auckland Park, Johannesburg, 2000. 1998.
3. Esterhuizen, E. Improved support design through a keyblock approach. Interim Report for SIMRAC Project GAP 330, Stope face support systems, prepared by CSIR Mining Technology and University of Pretoria, 1998. pp. 1–83.
4. Roberts, M.K.C. Stope and gully support. Final Report for SIMRAC Project GAP 032, CSIR Mining Technology. 1995. pp. 1–45.
5. Rockfield, ELFEN User Manual, Version 2.6, University College of Swansea. 1996.
6. Jager, A.J. and Roberts, M.K.C. Support systems in productive excavations. Gold 100. *Proc. of the Int. Conf. on Gold*. vol. 1: Gold Mining Technology. SAIMM, Johannesburg. 1986. pp. 289–300.
7. Squelch, A.P. The determination of the influence of backfill on rockfalls in South African gold mines. M.Sc. dissertation, University of Witwatersrand, Johannesburg. 1994.

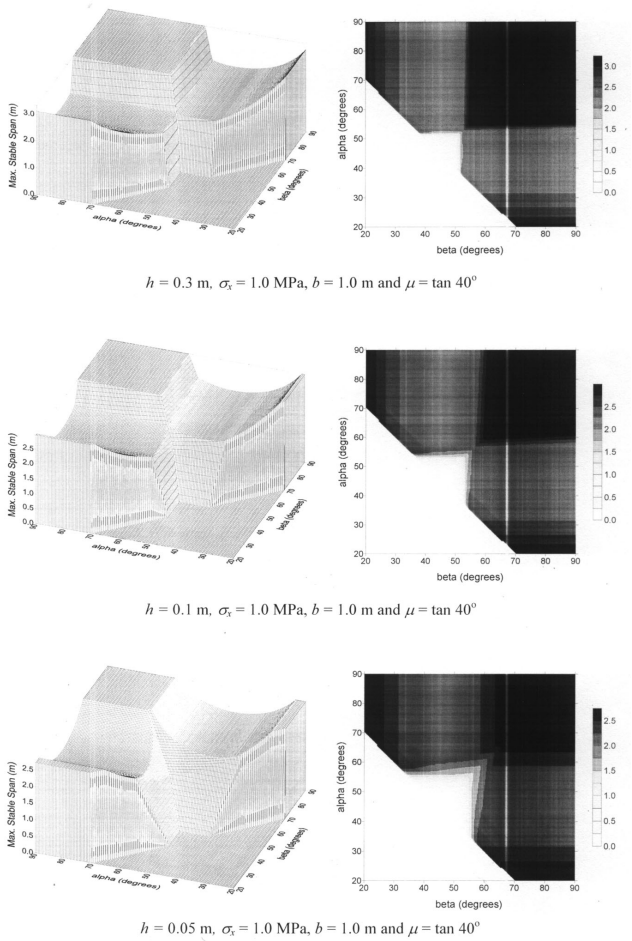

Figure 28—Output of the rockburst support design methodology; effect of various hangingwall arrest distances (*h*)

8. Herrmann, D.A. Fracture control in the hangingwall and the interaction between the support system and the overlying strata. M.Sc. dissertation, University of Witwatersrand, Johannesburg. 1987.
9. Evans, W.H. The strength of undermined strata. *Trans Instn Min. Metall.* 50. 1941. pp. 475–532.
10. Beer, G. and Meek, J.L. Design curves for roofs and hangingwalls in bedded rock based on voussoir beam and plate solutions. *Trans Instn Min. Metall.* 91. 1982. pp. A18–22.
11. Brady, B.H.G. and Brown, E.T. Rock Mechanics for Underground Mining. *George Allen and Unwin*. 1985. pp. 214–218.
12. Hutchinson, D.J. and Diederichs, M.S. Cablebolting in Underground Mines. *BiTech Publishers*. 1996. pp. 265–269.
13. Bandis, S.C., Lumsden, A.C. and Barton, N.R. Fundamentals of rock joint deformation. *Int. J. Rock Mech. Min. Sci. and Geomech*. Abstr. 20(6). 1983. pp. 249–268.
14. Daehnke, A., Andersen, L.M., de Beer, D., Esterhuizen, G.S., Glisson, F.J., Grodner, M.W., Hagan, T.O., Jaku, E.P., Kuijpers, J.S., Peake, A.V., Piper, P.S., Quaye, G.B., Reddy, N., Roberts, M.K.C., Schweitzer, J.K., Stewart, R.D., and Wallmach, T. Stope face support systems. Final Report for SIMRAC Project GAP 330, CSIR Mining Technology. 1998. pp. 1–407.
15. Kirsten, H.A.D. and Stacey, T.R. Hangingwall behaviour in tabular stopes subjected to seismic events. *J. S. Afr. Inst. Min. Metall.*, 88(5). 1988. pp. 163–172.
16. Ortlepp, W.D. High ground displacement velocities associated with rockburst damage. *Proc. 3rd Int. Symp. On Rockbursts and Seismicity in Mines*, Kingston, Ontario, Canada, 16–18 Aug., 1993. pp. 101–106.
17. Daehnke, A. Stress wave and fracture propagation in rock. Ph.D. thesis, Vienna University of Technology. 1997.
18. Wagner, H. Support requirements for rockburst conditions. *Proc. of the 1st Int. Cong. on Rockbursts and Seismicity in Mines*, SAIMM, eds. N.C. Gay and E.H. Wainwright, Johannesburg. 1984. pp. 209–218. ◆

Coal Indaba 2000*

The Fossil Fuel Foundation in association with The South African Institute of Mining and Metallurgy, The Geological Society of South Africa, and The Southern African Institute of Energy, will be presenting the 6th Coal Science and Technology Conference on 15 and 16 November, 2000 titled 'Changing trends in energy use from fossil fuel'. The conference which is being organized by Mintek, will be held at the Karos Indaba Hotel in Fourways.

The conference aims to bring to the attention of professionals, practitioners, and academics, in the energy and fossil fuel industries, up-to-date developments, trends, research and innovation relating to energy generation from fossil fuels. The first day will focus on coal characterization, geological benefication, utilization, and environmental aspects. The second day will cover the processing and utilization of coal and coal products for specific purposes, such as the metallurgical industries, power generation, and gasification.

Students will be particularly welcome, and are encouraged to present papers on their current research.

Opportunities will be available for supporting organizations to promote products and services, and a conference dinner will be held on the first evening.

Papers are invited, and abstracts no longer than 500 words should be sent to the Conference Secretariat at: *6th Indaba 2000, Mintek, Private Bag X3015, Randburg 2125, South Africa*.

Telephone and fax enquiries may be made to Yvonne Arnold and Jean Martins on (011) 709-4321/709-4326.

E-mail: yvonnea@mintek.co.za or jeanm@mintek.co.za. Website: http://members.xoom.com.FOSSIL FUEL. ◆

** Issued by: Patricia Speedie, Mintek, Private Bag X3015, Randburg, 2125, Tel: (011) 709-4111, Fax: (011) 709-4326*